

Mechanistic Insights into the Racemization of Fused Cyclopropyl Isoxazolines

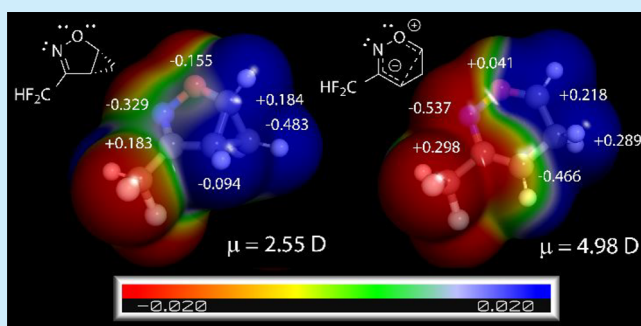
Kyle W. Quasdorf,^{*,†} Adam B. Birkholz,[†] Michael D. Bartberger,^{*,††} John Colyer,[†] Stephen Osgood,[†] Kevin Crossley,[†] and Seb Caille[†]

[†]Departments of Chemical Process Research and Development and Therapeutic Discovery, Amgen, Inc., One Amgen Center Drive, Thousand Oaks, California 91320, United States

^{††}1200 Pharma LLC, 844 East Green Street, Suite 204, Pasadena, California 91101, United States

Supporting Information

ABSTRACT: Experimental and computational studies of the unexpected racemization of enantiopure fused cyclopropyl isoxazolines are reported. These studies offer insights into the mechanism of racemization, quantify the position of the transition state on the dipolar–diradical continuum, and establish a relationship between the structure and stability of this class of compounds. Experimental and computed energy barriers for racemization are also presented.



Since the discovery that aspartyl protease BACE was shown to lead to the increased formation of β -secretase cleavage products,¹ the pursuit of a BACE inhibitor compound has been an important area of research over the past decades as a potential treatment for Alzheimer's disease.² AMG 978 (4) emerged as a lead compound from our BACE program, with the key step in the synthetic sequence being the diastereoselective addition of aryl lithium compound 2 to cyclopropyl fused isoxazoline 1, as shown in Figure 1.³ This

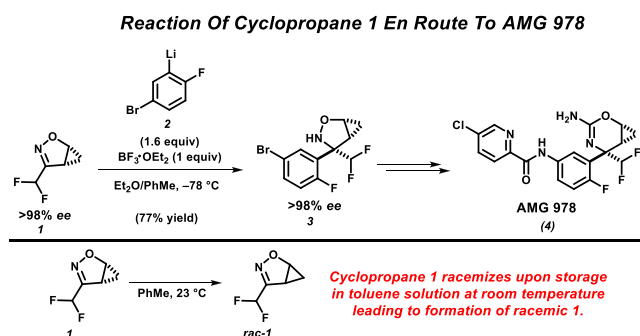


Figure 1. Reaction and racemization of cyclopropane 1.

reaction typically proceeds in good yield producing 3 in high diastereomeric ratio (dr) and enantiomeric excess (ee). Having access to enantiopure cyclopropane 1 is essential for being able to ultimately deliver 4 with the required chemical and optical purity. However, during our process development efforts for this reaction, we observed an erosion of ee in various lots of AMG 978 over several batches, and, eventually, only racemic 4

was obtained. After conducting a series of control experiments, it was discovered that batches of enantiopure cyclopropane 1 had, in fact, completely racemized upon being stored as solutions in toluene under ambient conditions at room temperature.

There have been several reports describing the synthesis of fused cyclopropyl isoxazolines,⁴ including enantioenriched variants,⁵ and, to the best of our knowledge, the susceptibility of these compounds to racemization has not been reported. We considered the fragmentation of the central carbon–carbon bond of the cyclopropane as the most likely source for this mode of racemization, as shown in Figure 2.

We envisioned that the racemization could potentially occur through a dipolar, zwitterionic pathway (Figure 2, top), involving heterolytic cleavage of the cyclopropane carbon–

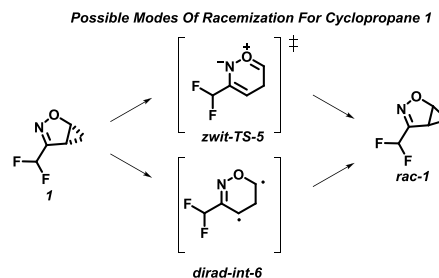


Figure 2. Possible zwitterionic or diradical pathways for racemization of 1 to rac-1.

Received: November 25, 2019

carbon bond, proceeding through transition structure **zwit-TS-5** with or without the presence of an intermediate along the potential surface. An alternative pathway (Figure 2, bottom) would involve homolytic opening of the cyclopropane through a diradicaloid TS to form diradical intermediate **dirad-int-6** and subsequent ring closure. Note that rearrangement of the all-carbon bicyclo[3.1.0]hex-2-ene substrate has been studied experimentally⁶ by the Baldwin and Doering groups, and, more recently, computationally by Houk,⁷ establishing the diradical pathway as the dominant mode of isomerization.

Given the overall structural similarity, yet potential electronic differences between our fused cyclopropyl isoxazolines and the parent hydrocarbon, a series of control experiments and computational investigations were conducted. Key experimental findings were as follows: (i) the rate of racemization was increased at higher temperatures; (ii) the rate of racemization was increased as the solvent dielectric constant increased; (iii) the presence of oxygen or light had no effect on the rate of racemization; and (iv) the inclusion of radical inhibitors such as BHT had no effect on the rate of racemization. While dipolar intermediates such as **zwit-TS-5** are known to react with dipolarophiles,⁸ the addition of species such as styrene or methyl acrylate did not allow for the trapping of any adducts arising from dipolar cycloadditions. In fact, throughout all of our control experiments, no side products were observed whatsoever.

Our initial computational imperative was to characterize the structural and electronic nature (zwitterionic versus diradical, presence of intermediates, etc.) of the racemization process depicted in Figure 2. All calculations were performed using the Gaussian 16 program.⁹ To begin, CASSCF(4,4)/6-31+G* calculations with an active space analogous to the previously studied hydrocarbon (C=N π/π^* and cyclopropyl-like σ/σ^*) were utilized to locate a TS for the racemization of **1**. This TS is structurally characterized by a flattening of the out-of-plane methylene with concomitant lengthening of the breaking C–C σ -bond, along with the equalization of the C=N and C–C ring bonds constituting the “aza-allyl” moiety at the TS, versus the corresponding distances in the reactant. IRC calculations originating from this transition structure progress smoothly to product or reactant without the presence of intermediates along the reaction path.

In contrast to the bicyclo[3.1.0]hex-2-ene archetype, the (4,4) CAS occupancies of the transition state for the racemization of **1** were found to be 1.92, 1.68, 0.32, and 0.08,¹⁰ descriptive of a process possessing a small amount of diradical character but predominantly closed-shell in nature. Furthermore, geometry optimization and stability calculations utilizing single-reference density functional theory (DFT) (R ω B97x-D/6-311+G(d,p); vide infra) resulted in a TS geometry with a stable closed-shell DFT solution. Finally, while a stable intermediate on the triplet diradical surface corresponding to **dirad-int-6** was located by DFT calculations, this species was found to be ~ 10 kcal/mol higher in energy than the analogous, closed-shell singlet TS at the same level of theory. Taken together, these data suggest that the racemization of **1** is best described as proceeding through a predominantly zwitterionic mechanism devoid of intermediates.

Having established the suitability of this system for study by single-reference methods, we then investigated the effect of implicit solvent on the description of reaction energetics, while also evaluating DFT functionals (selected based on the ability

to reproduce pericyclic reaction barrier heights in recent benchmarks^{11–13}) to determine which functional best models the experimental data. As discussed below, the ω B97x-D/6-311+G(d,p) model chemistry was ultimately utilized throughout the study. For **1**, the calculated barrier for racemization is found to diminish with increasing solvent dielectric (see Figure 3), in accord with experimental results (vide infra). Increasing

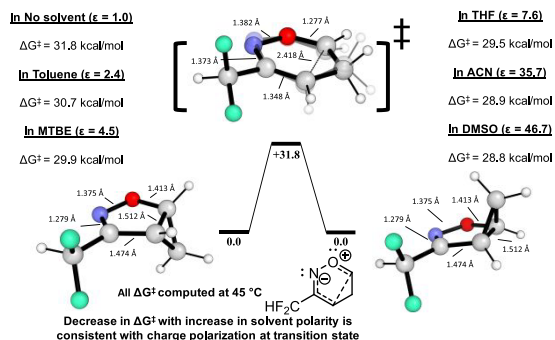


Figure 3. Computed geometric parameters (gas phase) and relative free energies of activation at 45 °C in various solvents for the racemization of **1** at the IEFPCM- ω B97x-D/6-311+G(d,p) level of theory. Semitransparent atoms at the transition structure illustrate motion along the imaginary frequency vibrational mode (see the Supporting Information for an animated graphic).

solvent dielectric was observed to stabilize the formation of a dipole at the transition state (as gauged by dipole moment magnitude relative to reactant, see the Supporting Information for details), as would be expected for a zwitterionic reaction mechanism.¹⁴ The electrostatic potential-derived charges exhibit clear differences between substrate **1** and its transition structure for racemization (Figure 4). In particular, the buildup

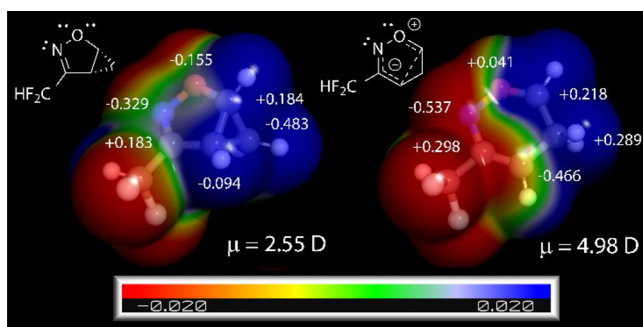


Figure 4. Electrostatic potential (a.u.) mapped onto the total electron density (0.001 a.u. contour level) with selected heavy atom Merz–Kollman atomic charges (electrons, fit to dipole moment; Debye) of substrate and TS of **1** ($\epsilon = 1$) illustrating the shift in charge distribution. ω B97x-D/6-311+G(d,p). Image rendered with PyMOL¹⁵

of a partial positive charge at the oxocarbenium-like oxygen atom and increased negative charge at the terminal C and N atoms of the aza-allyl-like moiety is readily evident.

We reasoned that the energetics of the reaction could be modulated by varying the functional group at the position of the difluoromethane unit present in cyclopropane **1**. As expected, electron-withdrawing groups that stabilize the nascent accumulation of overall negative partial charge at the aza-allyl moiety of the TS were predicted to lower the barrier for racemization, compared to those bearing substituents that

are more electron-donating. Utilizing the compounds shown in Figure 5, we set out to experimentally determine ΔG^\ddagger values and perform further studies on the racemization of these compounds.^{16,17}

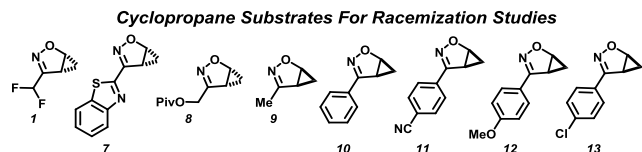
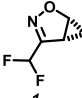


Figure 5. Cyclopropane substrates for racemization studies.

We began by studying the racemization of cyclopropane **1** in MTBE, acetone, and acetonitrile. The racemization rate is slowest in MTBE and occurs most rapidly in acetonitrile. This is consistent with our earlier observations and computational predictions that the rate of racemization increases as the solvent polarity increases. A comparison of the experimentally determined¹⁸ and computationally predicted ΔG^\ddagger values for the racemization of cyclopropane **1** in those solvents is shown in Table 1. There is excellent agreement in the solvent trends between the experimental and computational data.

Table 1. Experimental and Computational ΔG^\ddagger Values for Racemization of Cyclopropane **1** in Various Solvents at 30 °C^a

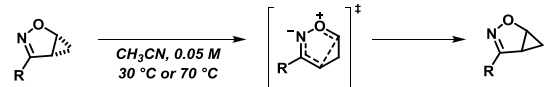
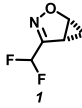
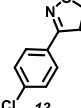
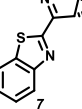
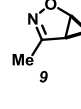
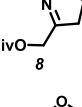
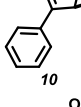
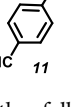
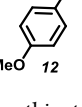
substrate	solvent	experimental ΔG^\ddagger values (kcal/mol)	calculated ΔG^\ddagger (kcal/mol) unshifted ¹	calculated ΔG^\ddagger (kcal/mol) shifted ^{1,2}
	MTBE	26.6	29.9	27.1
	Acetone	25.9	29.0	26.2
	Acetonitrile	25.6	28.9	26.1

^aNote the following footnotes cited in this table: ¹calculated using IEFPCM- ω B97x-D/6-311+G(d,p); and ²includes a correction of -2.7 kcal/mol, to account for observed systematic mean signed error in the DFT calculations.

Having explored the effects of solvent on cyclopropane **1**, we then set out to determine experimental ΔG^\ddagger values for each substrate shown in Figure 5, in order to compare to the computationally predicted value. For this study, with acetonitrile as the solvent of choice, temperatures of either 30 °C or 70 °C were selected, depending on the stability of the substrate. Experiments for substrates with lower barriers of racemization were conducted at 30 °C, and those with higher barriers were performed at 70 °C. All of the tested DFT functionals showed good correlation with experiment, giving free-energy R^2 values of >0.95 (see the Supporting Information) but systematically underestimated or overestimated the barrier height by 2–5 kcal/mol, compared to experiment. CCSD(T)/aug-cc-pVTZ single-point calculations on cyclopropane **1** were performed using the ω B97x-D/6-311+G(d,p) geometries. The difference between the DFT barrier and the CCSD(T) barrier was approximately equal to the systematic error observed in the DFT calculations, relative to the experiment (see the Supporting Information for further discussion). Among the functionals tested, IEFPCM- ω B97x-D/6-311+G(d,p) gave the best combination of relative and absolute agreement with experiment and are used throughout this work. ($R^2 = 0.96$, slope = 1.10, 2.7 kcal/mol MUE, where MUE denotes mean unsigned error). The experimental and

calculated barrier heights are presented in Table 2, with the correlation highlighted in Figure 6.

Table 2. Experimental and Computational ΔG^\ddagger Values for Cyclopropane Substrates in Acetonitrile at 30 or 70 °C^a

					
entry	substrate	experimental ΔG^\ddagger calculated ΔG^\ddagger ^{1,2} (MSE shifted) ^{1,2,3}	entry	substrate	experimental ΔG^\ddagger calculated ΔG^\ddagger ^{1,2} (MSE shifted) ^{1,2,3}
1		25.6 ⁴ 28.9 ⁴ 26.1 ⁴	5		29.0 ⁵ 31.7 ⁵ 29.0 ⁵
2		26.4 ⁴ 29.0 ⁴ 26.3 ⁴	6		29.5 ⁵ 31.6 ⁵ 28.8 ⁵
3		27.8 ⁴ 30.8 ⁴ 28.0 ⁴	7		29.5 ⁵ 32.1 ⁵ 29.4 ⁵
4		28.5 ⁵ 31.0 ⁵ 28.4 ⁵	8		29.8 ⁵ 32.6 ⁵ 29.9 ⁵

^aNote the following footnotes cited in this table: ¹ ΔG^\ddagger values reported in units of kcal/mol. ²IEFPCM- ω B97x-D/6-311+G(d,p); ³values shifted by -2.7 kcal/mol for observed systematic error; ⁴measured and calculated at 30 °C; and ⁵measured and calculated at 70 °C.

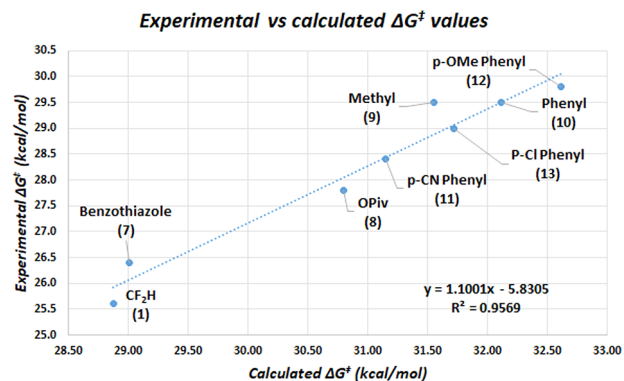


Figure 6. Comparison between experimental and calculated ΔG^\ddagger values for the eight cyclopropane substrates in acetonitrile.

The difluoromethane, benzothiazole, and pivalate substrates (entries 1, 2, and 3, respectively, in Table 2) possess experimentally measured ΔG^\ddagger values of 25.6, 26.4, and 27.8 kcal/mol at 30 °C. The (comparatively less electron-withdrawing) methyl- and aryl-substituted compounds proved to be significantly more stable. Thus, the racemization of these compounds was performed at 70 °C in order to achieve reasonable rates. The *p*-CN phenyl substrate exhibited the most facile racemization of this group, with an experimentally

determined ΔG^\ddagger value of 28.5 kcal/mol (Table 2, entry 4) followed by the *p*-Cl substrate (Table 2, entry 5) at 29.0 kcal/mol. The methyl and phenyl substrates had almost identical stabilities, with both compounds having a measured ΔG^\ddagger value of ~29.5 kcal/mol (Table 2, entries 6 and 7). Finally, the *p*-OMe phenyl substrate proved to be the most stable substrate investigated, with an experimental racemization energy barrier of 29.8 kcal/mol (Table 2, entry 8). All experimentally determined ΔG^\ddagger values demonstrate an excellent correlation with computationally determined ΔG^\ddagger values, as highlighted in Table 2 and Figure 6.

To further support the proposed dipolar mechanism, a Hammett plot was constructed from data collected for the *p*-OMe phenyl, phenyl, *p*-Cl phenyl, and *p*-CN phenyl substituted cyclopropane compounds, as shown in Figure 7.¹⁹ The slope of the Hammett plot is consistent with buildup

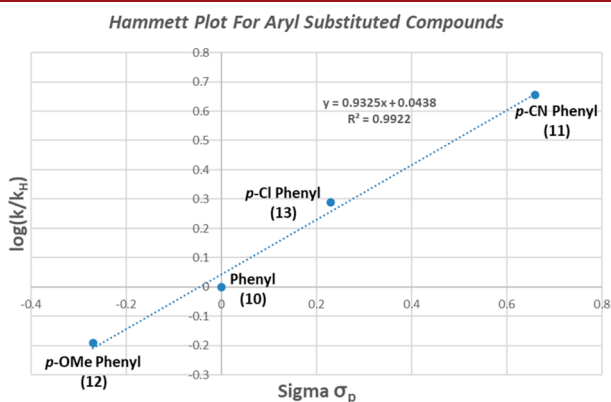


Figure 7. Hammett plot for aryl-substituted cyclopropanes.

of a negative charge (i.e., the existence of a partial aza-allyl-like anion moiety) in the transition state for racemization. The highly linear nature of the plot is supportive of a consistent mode of racemization over a range of electronically diverse substrates.

In conclusion, we have performed both experimental and computational studies on the unexpected racemization of enantiopure cyclopropyl fused isoxazoline compounds. Both the experimental and computational data are consistent with the racemization proceeding primarily through a transition state possessing predominantly dipolar character. The stability of these compounds can be significantly modulated by temperature, choice of solvent, and substituents.

■ ASSOCIATED CONTENT

§ Supporting Information

The Supporting Information is available free of charge at <https://pubs.acs.org/doi/10.1021/acs.orglett.9b04236>.

Experimental procedures, characterization data, and computational data (PDF)

■ AUTHOR INFORMATION

Corresponding Authors

*E-mail: quasdorf@amgen.com (K. W. Quasdorf).

*E-mail: michael.bartberger@1200pharma.com (M. D. Bartberger).

ORCID 

Michael D. Bartberger: 0000-0002-5167-3139

Seb Caille: 0000-0001-5434-5483

Notes

The authors declare no competing financial interest.

■ ACKNOWLEDGMENTS

Stimulating discussions with Drs. Jason Tedrow and Narbe Mardirossian (Amgen, Inc.) are gratefully acknowledged.

■ REFERENCES

- (1) Vassar, R.; Bennett, B.; Babu-Khan, S.; Khan, S.; Mendiaz, E.; Denis, P.; Teglou, D.; Ross, S.; Amarante, P.; Loeloff, R.; Luo, Y.; Fisher, S.; Fuller, J.; Edenson, S.; Lile, J.; Jarosinski, M.; Biere, A.; Curran, E.; Burgess, T.; Louis, J.-C.; Collins, F.; Treanor, J.; Rogers, G.; Citron, M. *Science* **1999**, *286*, 735–741.
- (2) Low, J. D.; Bartberger, M. D.; Cheng, Y.; Whittington, D.; Xue, Q.; Wood, S.; Allen, J. R.; Minatti, A. E. *Bioorg. Med. Chem. Lett.* **2018**, *28*, 1111–1115.
- (3) Uno, H.; Terakawa, T.; Suzuki, H. B. *Bull. Chem. Soc. Jpn.* **1993**, *66*, 2730–2737.
- (4) (a) Burrows, T. G.; Jackson, W. R.; Faulks, S.; Sharp, I. *Aust. J. Chem.* **1977**, *30*, 1855–1858. (b) Sheshenev, A. E.; Baird, M. S.; Bolesov, I. G.; Shashkov, A. S. *Tetrahedron* **2009**, *65*, 10552–10564. (c) Nesi, R.; Giomi, D.; Papaleo, S.; Dapporto, P.; Paoli, P. *J. Chem. Soc., Chem. Commun.* **1990**, *23*, 1675–1676. (d) Baird, M. S.; Li, X.; Al Dulayymi, J. R.; Kurdjukov, A. I.; Pavlov, V. A. *J. Chem. Soc., Perkin Trans. 1* **1993**, *21*, 2507–2508.
- (5) Baird, M. S.; Huber, F. A. M.; Clegg, W. *Tetrahedron* **2001**, *57*, 9849–9858.
- (6) (a) Baldwin, J. E.; Keliher, E. J. *J. Am. Chem. Soc.* **2002**, *124*, 380–381. (b) von E. Doering, W.; Zhang, T.-h.; Schmidt, E. K. G. *J. Org. Chem.* **2006**, *71*, 5688–5693.
- (7) (a) Suhrada, C. P.; Houk, K. N. *J. Am. Chem. Soc.* **2002**, *124*, 8796–8797. (b) Doubleday, C.; Suhrada, C. P.; Houk, K. N. *J. Am. Chem. Soc.* **2006**, *128*, 90–94.
- (8) Partridge, K. M.; Guzei, I. A.; Yoon, T. P. *Angew. Chem., Int. Ed.* **2010**, *49*, 930–934.
- (9) Frisch, M. J.; Trucks, G. W.; Schlegel, H. B.; Scuseria, G. E.; Robb, M. A.; Cheeseman, J. R.; Scalmani, G.; Barone, V.; Petersson, G. A.; Nakatsuji, H.; Li, X.; Caricato, M.; Marenich, A. V.; Bloino, J.; Janesko, B. G.; Gomperts, R.; Mennucci, B.; Hratchian, H. P.; Ortiz, J. V.; Izmaylov, A. F.; Sonnenberg, J. L.; Williams-Young, D.; Ding, F.; Lipparini, F.; Egidi, F.; Goings, J.; Peng, B.; Petrone, A.; Henderson, T.; Ranasinghe, D.; Zakrzewski, V. G.; Gao, J.; Rega, N.; Zheng, G.; Liang, W.; Hada, M.; Ehara, M.; Toyota, K.; Fukuda, R.; Hasegawa, J.; Ishida, M.; Nakajima, T.; Honda, Y.; Kitao, O.; Nakai, H.; Vreven, T.; Throssell, K.; Montgomery, J. A., Jr.; Peralta, J. E.; Ogliaro, F.; Bearpark, M. J.; Heyd, J. J.; Brothers, E. N.; Kudin, K. N.; Staroverov, V. N.; Keith, T. A.; Kobayashi, R.; Normand, J.; Raghavachari, K.; Rendell, A. P.; Burant, J. C.; Iyengar, S. S.; Tomasi, J.; Cossi, M.; Millam, J. M.; Klene, M.; Adamo, C.; Cammi, R.; Ochterski, J. W.; Martin, R. L.; Morokuma, K.; Farkas, O.; Foresman, J. B.; Fox, D. J. *Gaussian 16*, Revision C.01; Gaussian, Inc.: Wallingford, CT, 2016.
- (10) (a) CAS occupancies at CASSCF (4,4)/6-31+G* for 2-difluoromethyl-bicyclo[3.1.0]hex-2-ene were found to be 1.91, 1.01, 0.99, and 0.09. (b) Inclusion of oxygen lone pairs in the active space (i.e., CASSCF (6,5) for the transition structure for racemization of 1) does not significantly change the form of the CAS orbitals nor the observed CAS occupancies. See the Supporting Information for an elaborated discussion.
- (11) Goerigk, L.; Hansen, A.; Bauer, C.; Ehrlich, S.; Najibi, A.; Grimme, S. *Phys. Chem. Chem. Phys.* **2017**, *19*, 32184–32215.
- (12) Mardirossian, M.; Head-Gordon, M. *Mol. Phys.* **2017**, *115*, 2315–2372.
- (13) See the Supporting Information for further details on the computational results.

(14) Reichardt, C.; Welton, T. *Solvents and Solvent Effects in Organic Chemistry*; Wiley–VCH Verlag & Co. KGaA, Weinheim, Germany, 2011.

(15) *The PyMOL Molecular Graphics System*, Version 2.1.1; Schrödinger, LLC.

(16) For compounds **1**, **7**, and **8**, absolute stereochemistry was established from an advanced intermediate in the AMG 978 synthesis. For compounds **9**, **10**, **11**, **12**, and **13** absolute stereochemistry was determined by comparison to known literature compounds. See the [Supporting Information](#) for details.

(17) Sakai, T.; Mitsutomi, H.; Korenaga, T.; Ema, T. Enantio-enriched aryl substrates were obtained via an enzymatic resolution. *Tetrahedron: Asymmetry* **2005**, *16*, 1535–1539.

(18) See the [Supporting Information](#) for details on the experimental determination of ΔG^\ddagger values.

(19) Hansch, C.; Leo, A.; Taft, R. W. *Chem. Rev.* **1991**, *91*, 165–195.